Quantum interference with distinguishable photons through indistinguishable pathways

Yoon-Ho Kim

Department of Physics, Pohang University of Science and Technology (POSTECH), Pohang 790-784, South Korea

Warren P. Grice

Center for Engineering Science Advanced Research, Computer Science and Mathematics Division, Oak Ridge National Laboratory, Oak Ridge, Tennessee 37831

Received April 8, 2004; revised manuscript received July 9, 2004; accepted September 19, 2004

We report a two-photon quantum interference experiment in which the detected individual photons have quite different properties. The interference is observed even when no effort is made to mask the distinguishing features before the photons are detected. The results can be explained only in terms of indistinguishable two-photon amplitudes. © 2005 Optical Society of America

OCIS codes: 270.0270, 270.1670.

1. INTRODUCTION

Quantum mechanical interference is observed when an event can occur by any of several alternative pathways. If an experiment is performed in which it is possible to determine which of the alternative pathways was actually taken, then the interference is lost.[1,2] For two-photon interference, the existence of indistinguishable alternative pathways for a pair of detection events leads to the interference. One of the best-known examples is the Hong–Ou–Mandel interferometer, in which two identical photons meet at a 50/50 beam splitter and two single-photon detectors monitor the rate at which both detectors register photons[3] (coincidence count). A coincidence count may be recorded either when both photons are reflected (r–r) or when both are transmitted (t–t). If the photons reach the beam splitter simultaneously, then these two pathways are indistinguishable, and interference is observed in the form of a photon bunching effect: The photons exit the beam splitter together, resulting in a null in the coincidence rate.[4,5]

Although the photons reaching the beam splitter in this example are identical, it is possible to observe interference even if the photons are distinguishable when they reach the beam splitter. The key is to detect the photons in such a way that the distinguishing information is masked.[6–8] If, for example, the input photons are orthogonally polarized, no interference is expected, since the polarizations of the detected photons would make it possible to distinguish the r–r and the t–t pathways. The interference is restored, however, when the photons are simply passed through polarizers before detection. With their pass axes oriented halfway between the polarizations of the two input photons, the polarizers mask the polarization information.[9–14] The same principles may be applied to distinguishing timing information. If the photons in one input port arrive earlier than their counterparts, then the r–r and t–t pathways are distinguishable by the photon arrival times, and no interference is observed. Again, the interference may be restored by masking the distinguishing timing information.[15] This may be accomplished, for example, by introducing alternate pathways into one of the exit ports.[14,16] The photon can reach the detector by one of two paths, leading to two different arrival times. If the delays are chosen properly, it is impossible to determine whether the photon left the beam splitter first and took the longer path to the detector or left later and reached the detector via the shorter path. It is also possible to mask the distinguishing timing information by using narrowband spectral filters that increase inherent uncertainties associated with the differences in the photon pair arrival times at the beam splitter.[17–19]

These examples illustrate the role of indistinguishability in quantum interference. If the photons are not indistinguishable in all respects when they reach the beam splitter, then elements must be introduced to mask the distinguishing information, in effect rendering the distinguishable photons indistinguishable. Here, we report an interference experiment in which the detected photons retain their distinguishing information. The photons approach the beam splitter at different times, with different polarizations, and may even have different wavelengths. They propagate directly to the detectors without passing through compensating or masking elements and retain their distinguishing properties until being absorbed by the detectors. Nonetheless, interference is observed in the coincidence rate. We explain this counterintuitive result as the interference between two two-photon wave packets.

2. EXPERIMENT

An outline of the experimental setup is shown in Fig. 1. A 3-mm-thick type II beta barium borate (BBO) crystal is

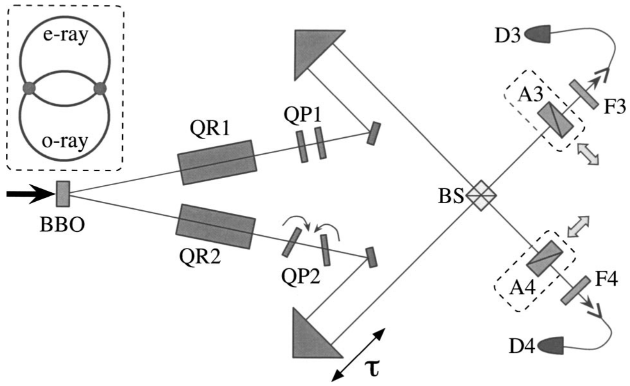

Fig. 1. Experimental setup. Orthogonally polarized photon pairs are generated from the BBO crystal by type II spontaneous parametric downconversion. Polarization analyzers A3 and A4 are removable. QR1, QR2, quartz rods; QP1, QP2, quartz plates; BS, beam splitter, D3, D4, detectors; F3, F4, filters.

pumped by a train of ultrafast pulses with central wavelength of 390 nm and pulse duration of approximately 120 fs. The crystal is oriented so that a small fraction of the pump photons are downconverted by the process of spontaneous parametric downconversion (SPDC) to orthogonally polarized signal and idler photons with center wavelengths of 780 nm. The downconverted photons are emitted into two distinct cones, one with extraordinary polarization (V polarized) and the other with ordinary polarization (H polarized). Here we are interested in the intersections of the two light cones, where the polarizations of the single photons cannot be defined.[20–26] These two directions, defined by a set of apertures, form an angle of ± 3 degrees with respect to the pump propagation direction; see the inset of Fig. 1. These two spatial modes are directed by mirrors to the two input ports of an ordinary nonpolarizing beam splitter. The output ports are monitored by single-photon counting detectors, D3 and D4. Broadband (20 nm at FWHM) spectral filters, F3 and F4, preceding the detectors help to reduce background noise. Polarization analyzers A3 and A4 are removable so that the interference effect can be studied both with and without the polarizers in place.

A set of quartz rods and quartz plates are inserted into each arm of the interferometer: QR1 and QR2 are 20-mm-long quartz rods, and QP1 and QP2 are 600-μm-thick quartz plates. With their optic axes oriented vertically, these birefringent elements introduce a group delay of roughly 668 fs between the V- and the H-polarized photons in addition to the delay accumulated in the SPDC crystal. By tilting quartz plates QP2 about their optic axes, it is possible to introduce an additional fine delay between the orthogonally polarized photons. The delay between the two arms of the interferometer is controlled by a trombone prism attached to a computer-controlled dc motor. The count rates of the two detectors, as well as the rate of coincidences, were recorded as a function of the delay between the two arms of the interferometer. The effective coincidence window used in this experiment was $\sim$3 ns, which is smaller than the pump pulse repetition period ($\approx$13 ns).

Quantum interference is observed as the delay between the two arms is adjusted. This can be seen as the peak and dip shown in Fig. 2. The two different data sets correspond to two different phase settings, i.e., two different orientations of quartz plates QP2. Tilting the quartz plates introduces a subwavelength delay between the orthogonally polarized modes in the lower arm. The peak–dip phase is associated with this additional birefringent delay. Tilting the quartz plates increases not only the relative delay but also the total path length for the two different polarizations. This is reflected as an offset between the peak and the dip.

We note here that the two photons approach the beam splitter with quite different properties: they are orthogonally polarized and approach at different times (one photon always reaches the beam splitter 668 fs earlier than the other). This time delay is larger than both the 120-fs pump pulse duration and the 100-fs single-photon wave packet defined by the 20-nm (at FWHM) filter. It is somewhat surprising, then, that high-visibility interference is observed even though the photons' properties are not altered before the detection process, i.e., no elements are introduced after the beam splitter to mask the distinguishing information. (For instance, 45°-oriented polarizers and a group delay scheme could be used to erase the polarization and the temporal distinguishing information, respectively.)

To emphasize that quantum interference is indeed achieved with distinguishable photons, the experiment was repeated with polarizers A3 and A4 placed in front of the detectors. One of the polarizers was aligned to pass horizontally polarized light (A3 90°), while the other was aligned to pass vertically polarized light (A4 0°). The only photons that may be detected in such a setup are emitted and detected with orthogonal polarizations and are orthogonally polarized at every point in the interferometer. Nevertheless, high visibility quantum interference is observed, as shown in Fig. 3. Although the overall count rate is lowered, the peak and dip features are still evident with no change in the visibility.

In fact, the peak–dip quantum interference is completely independent of the polarizer angles. With QP2 fixed for the coincidence peak (dip), the measurement was repeated for polarizer angles A3 45° and A4 −45° (orthogonal polarizers) and A3 45° and A4 45° (parallel po-

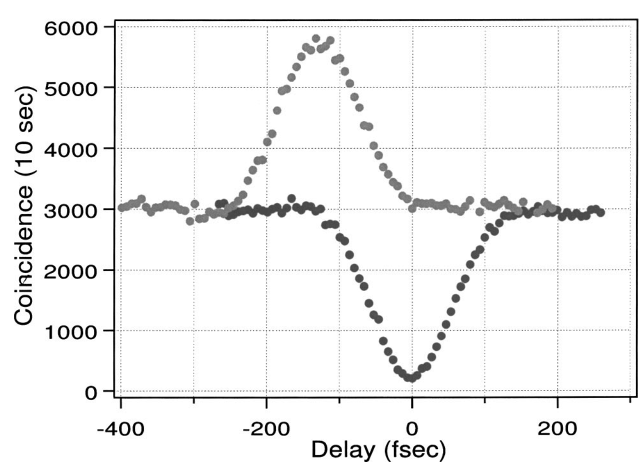

Fig. 2. Experimental data showing two-photon quantum interference. Polarization analyzers were not used for this measurement. The peak–dip visibility is $\sim$93%.

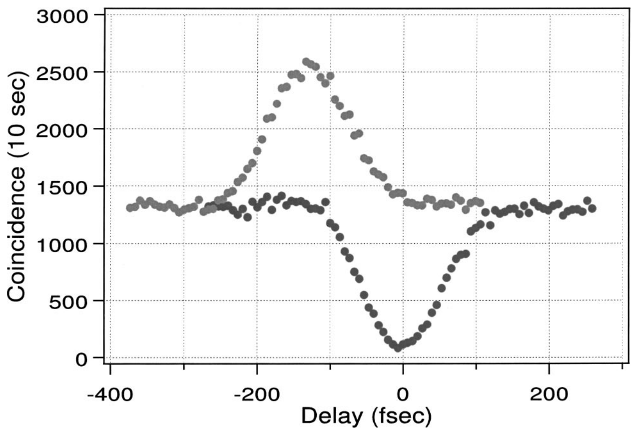

Fig. 3. Experimental data with polarizers A3 oriented at 90° and A4 at 0°. The visibility of the quantum interference remains the same, but the overall count rate has been reduced.

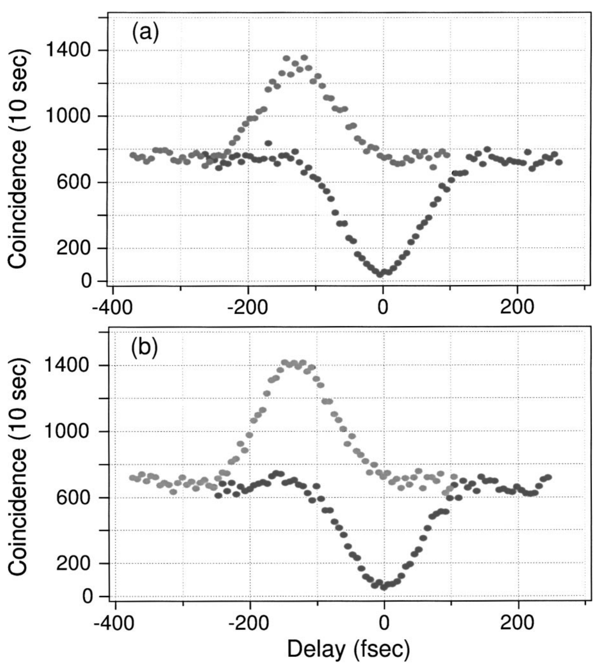

Fig. 4. Experimental data with (a) polarizer A3 at 45° and A4 at 45°, (b) polarizer A3 at 45° and A4 at −45°. The overall count rate has been reduced but the visibility remains the same.

larizers). These polarizer settings will typically change the coincidence peak (dip) into a coincidence dip (peak).[9–14] In this experiment, however, the peak structure remained, with no change in the visibility: only the overall count rates are reduced. Figure 4 shows the data for this set of measurements.

3. THEORY

The experimental results make it clear that it is possible to observe high-visibility quantum interference even when the detected photons have quite different properties. The interference effect can be understood more clearly through a calculation of the coincidence rate at the two detectors. As described above, the photons leave the SPDC crystal in the paths corresponding to the overlap of the o- and the e-polarized cones. The two-photon state may be written in this case as

$$|\Psi\rangle = \frac{1}{\sqrt{2}}[|\psi_{HV}\rangle + \exp(i\phi)|\psi_{VH}\rangle], \tag{1}$$

where $|\psi_{HV}\rangle$ and $|\psi_{VH}\rangle$ represent the two ways in which a photon pair may be emitted into these directions and where ϕ represents the phase between the two terms. Because the crystal is aligned for type II SPDC and because it is pumped by a train of short pulses, a multimode treatment is necessary to reveal the subtle spectral and temporal characteristics of the two-photon state.

Although the state may be described in either the spectral or the temporal domain, the analysis in this case is somewhat simpler in the temporal domain. Accordingly, the states $|\psi_{HV}\rangle$ and $|\psi_{VH}\rangle$ are

$$|\psi_{HV}\rangle = \iint \mathrm{d}t_o \mathrm{d}t_e \mathcal{G}_{HV}(t_o, t_e)\hat{a}^\dagger_{H1}(t_o)\hat{a}^\dagger_{V2}(t_e)|0\rangle,$$

$$|\psi_{VH}\rangle = \iint \mathrm{d}t_o \mathrm{d}t_e \mathcal{G}_{VH}(t_o, t_e)\hat{a}^\dagger_{V1}(t_e)\hat{a}^\dagger_{H2}(t_o)|0\rangle,$$

where the two-photon amplitude is given by

$$\begin{aligned}\mathcal{G}_{\mathrm{HV}}(t_o, t_e) &= \mathcal{G}_{VH}(t_o, t_e)\\ &= N\exp[-i\bar{\omega}(t_o + t_e)]\xi(t_o, t_e)\\ &\quad\times \Pi[t_e - t_o; 0, L(k_o' - k_e')].\end{aligned}$$

Here N is a normalization constant, $\bar{\omega}$ is the mean photon frequency, L is the crystal length, and the function $\Pi[t; t_1, t_2]$ is given by

$$\Pi[t; t_1, t_2] = \begin{cases} 1 & \text{for } t_1 < t < t_2 \\ 0 & \text{otherwise} \end{cases}. \tag{2}$$

The function $\xi(t_o, t_e)$ is related to the pump field and the birefringent properties of the crystal. For a pump field proportional to $\exp\{-[(\omega - 2\bar{\omega})/\sigma]^2\}$, $\xi(t_o, t_e)$ is

$$\xi(t_o, t_e) = \exp\left\{-\frac{\sigma^2}{4}\left[\left(\frac{k_p' - k_e'}{k_o' - k_e'}\right)t_o - \left(\frac{k_p' - k_o'}{k_o' - k_e'}\right)t_e\right]^2\right\},$$

where

$$k_p' = \left.\frac{\mathrm{d}k_p}{\mathrm{d}\omega}\right|_{2\bar{\omega}}, \qquad k_{o(e)}' = \left.\frac{\mathrm{d}k_{o(e)}}{\mathrm{d}\omega}\right|_{\bar{\omega}}$$

are the inverse group velocities of the pump (p) and the o-polarized (o) and e-polarized (e) photons, respectively.

Expressed in this way, it is easy to see that the two-photon probability amplitude describes a pair of photons whose emission times are determined primarily by the temporal shape of the pump pulse, modified somewhat by the group-velocity differences inside the crystal. The rectangle function $\Pi[t; t_1, t_2]$ sets upper and lower bounds for the difference in emission times and reflects the fact that the o- and the e-polarized photons will separate temporally as they propagate through the crystal. With a lower bound of zero (for a pair created at the exit face) and an upper bound of $L(k_o' - k_e')$ (for a pair created at the entrance face), it is evident that these expressions describe the two-photon states as they exit the crystal, i.e., before the photons pass through any birefringent elements.

After exiting the crystal, the photons propagate along paths 1 and 2, experiencing nearly identical birefringent delays (due to the quartz rods and quartz plates). They are then brought together at a beam splitter, though the path lengths may be slightly different. To within a constant overall phase, the two-photon state at the input of the beam splitter is simply the state given in Eq. (1) with the temporal arguments shifted as follows:

$$\mathcal{G}_{HV}(t_o, t_e) \rightarrow \mathcal{G}_{HV}(t_o, t_e - \tau_2 - \tau),$$

$$\mathcal{G}_{VH}(t_o, t_e) \rightarrow \mathcal{G}_{VH}(t_o - \tau, t_e - \tau_1).$$

Here, $c\tau$ is the difference in free-space path lengths between the upper and the lower paths. Delays τ_1 and τ_2 represent the delays of the e-polarized photons with respect to the o-polarized photons in paths 1 and 2, respectively.

With no polarizers in place, the coincidence rate at detectors D3 and D4 is given by

$$R = \int\int \mathrm{d}t\mathrm{d}t'[P_{HV}(t, t') + P_{VH}(t, t')], \tag{3}$$

where $P_{HV}(t, t')$ $[P_{VH}(t, t')]$ is the probability that a horizontally [vertically] polarized photon is detected at D3 at time t and that a vertically [horizontally] polarized photon is detected at D4 at time t'. The expression should in general also include the terms $P_{HH}(t, t')$ and $P_{VV}(t, t')$, but since the photons emitted in type II SPDC are orthogonally polarized, these are zero for the experiment described here.

The two-time detection probabilities are given by

$$P_{ij}(t, t') = |\langle 0|\hat{a}_{i3}(t)\hat{a}_{j4}(t')|\Psi\rangle|^2,$$

where i and j are the polarization labels, which can be H or V depending on the polarization state of the photon in a given spatial mode. To within a constant phase factor, the annihilation operators at the detectors are related to the input operators by

$$\hat{a}_{i3}(t) = \frac{1}{\sqrt{2}}[\hat{a}_{i2}(t) + i\hat{a}_{i1}(t)],$$

$$\hat{a}_{i4}(t) = \frac{1}{\sqrt{2}}[\hat{a}_{i1}(t) + i\hat{a}_{i2}(t)].$$

From the expressions given above, the coincidence count rate R given in Eq. (3) is found to be

$$\begin{aligned} R = R_0\Bigg(1 - \cos[\phi - \bar{\omega}(\tau_2 - \tau_1)]\left[1 - \frac{|2\tau + \tau_2 - \tau_1|}{L(k_o' - k_e')}\right] \\ \times \exp\left\{-\frac{\sigma^2}{8}\left[\left(\frac{2k_p' - k_o' - k_e'}{k_o' - k_e'}\right)\tau \right.\right. \\ \left.\left. + \left(\frac{k_p' - k_o'}{k_o' - k_e'}\right)(\tau_2 - \tau_1)\right]^2\right\} \\ \times \Pi[2\tau + \tau_2 - \tau_1; -L(k_o' - k_e'), L(k_o' - k_e')]\Bigg), \end{aligned} \tag{4}$$

where R_0 is a constant. Although this expression is a bit cumbersome, it is simplified greatly for $\tau = 0$ (equal path lengths) and $\tau_1 - \tau_2 \approx 0$ (nearly identical birefringent delays), in which case the expression becomes

$$R \approx R_0\{1 - \cos[\phi - \bar{\omega}(\tau_2 - \tau_1)]\}. \tag{5}$$

In this form it is clear that the coincidence count rate can be made to vanish for the appropriate birefringent delays and, likewise, that it can be raised to twice the background rate with a small phase shift. [Recall that ϕ is the unknown fixed phase term from Eq. (1).] It is these two settings that were used to generate the data shown in Figs. 2–4. As described above, the phase shift in $\tau_1 - \tau_2$ was introduced in our experiment by tilting QP2. This type of adjustment introduces slightly different path length increases for the two polarizations but also increases the overall length of the lower arm (of the interferometer) so that the trombone prism must be adjusted to compensate. This is the origin of the offset between the coincidence peak and the coincidence dip observed in the figures.

4. DISCUSSIONS

A couple of results from the above analysis invite further comment. First, the interference features are independent of the presence of polarizers or, if polarizers are in place, of their orientations. This is in contrast to previous experiments, in which the relative orientations of the polarizers determine the phase between the interfering terms and whether the interference is constructive or destructive. The inclusion of polarizers in the above analysis changes the overall rate of coincidence detection, but the peak–dip features persist. Thus, photon polarization has absolutely no bearing on the interference effect, and there is no need to mask differences between the photons' polarizations.

Another result worth noting is that the photons may reach the beam splitter at different times.[15] Recall that the photons are emitted with orthogonal polarizations and therefore travel at different speeds through the birefringent elements. By adjusting the birefringent delays, it is possible to change the arrival times for the orthogonally polarized photons. For maximum visibility, τ_1 and τ_2 must be nearly identical, but the constraint is on their difference, not on the individual delays. Thus interference can be observed for arbitrary amounts of birefringent delay, as long as the delays in the two arms are nearly identical. These results stand in contrast to previous works involving similar configurations, where interference could be observed only if there were no distinguishing timing or polarization information or if such information were erased before detection.[9–14,16,18,19,22–25] Here, such information seems not to matter.

The difference between those experiments and the one reported here is the input state. Whereas the previous experiments involved single two-photon states, the input state for our experiment is the superposition state of Eq. (1). This seemingly subtle change to the input state is critical to the observed interference effect, for this superposition now provides two pathways for a given detection outcome. Suppose, for example, that detector D3 registers a horizontally polarized photon while D4 registers a vertically polarized photon. There are two ways that this may happen: The photons may be emitted as $|H\rangle_1|V\rangle_2$ and be reflected at the beam splitter, or they may be emitted as $|V\rangle_1|H\rangle_2$ and be transmitted. As long as the interferometer is properly adjusted, these two pathways will be indistinguishable, even though the photons themselves may have quite different properties (see Ψ_1 and Ψ_4 in Fig. 5).

The relationships between the various detection pathways are shown in the two-photon Feynman diagrams of Fig. 5. The four diagrams leading to coincident detection correspond to two possible outcomes (both photons reflected, r–r, or transmitted, t–t, at the beam splitter) for each of the two possible emission states ($|H\rangle_1|V\rangle_2$ or $|V\rangle_1|H\rangle_2$). The four cases are pairwise indistinguishable: Ψ_1 and Ψ_4 correspond to H at D3 and V at D4, while Ψ_2 and Ψ_3 correspond to V at D3 and H at D4. Note, also, that the horizontally polarized photon is always detected first, a consequence of the birefringent delays. As long as the delays are identical, the amplitudes remain pairwise indistinguishable.

Returning to the comparison with previous two-photon interference experiments, it is clear that indistinguishability still plays an important role, even when the photons themselves are distinguishable. While the detected photons may be different, it is critical that the r–r and t–t pathways be indistinguishable. Typically, this condition could be satisfied only if the photons were identical as they entered the beam splitter or if they were detected in such a way that they appeared to be identical. Here the indistinguishability is found in the ambiguity of the input to the beam splitter. For example, a photon with a particular set of properties may be detected at a given detector, with a second photon having a distinct set of properties at the other detector. The r–r and t–t pathways remain indistinguishable, however, because there are two ways that these two photons may be emitted into the setup.

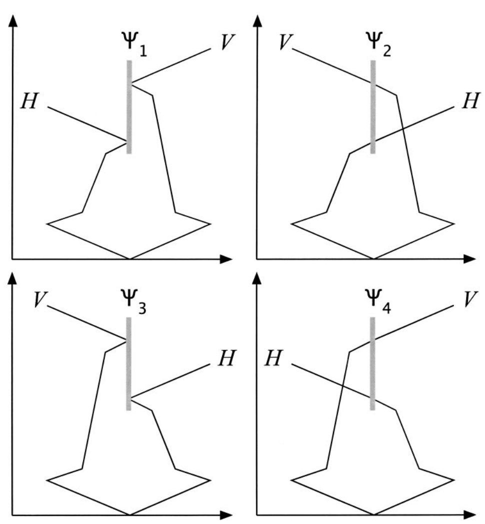

Fig. 5. Quantum mechanical two-photon Feynman alternatives. Ψ_1 and Ψ_4 are indistinguishable, and Ψ_2 and Ψ_3 are indistinguishable. As a result, quantum interference occurs pairwise and the interference peak–dip can be observed without needing to erase the actively distinguishing information. The vertical gray bar represents the beam splitter.

It is the superposition of the two two-photon states before they reach the beam splitter, therefore, that is essential to the interference effect. Indeed, this type of arrangement was originally proposed by Braunstein and Mann as a means of distinguishing one of the four polarization Bell states.[27,28] It is interesting to note that the interference effect persists even when $|\Psi\rangle$ exhibits little or no polarization entanglement. It is well documented that a pure polarization-entangled state may be generated only when the two photons in a particular path are distinguishable only by their polarizations. Differences in spectral properties or time of arrival tend to blur the entanglement.[22–26,29] In this experiment, however, the interference effect is observed even when the photons may be distinguished by their arrival times. Since the photon pairs are generated in an ultrafast-pulse-pumped type II crystal, they also posses distinguishing spectral information.[22–26,29,30] Even so, the visibility is much higher, 100% in principle, than would be expected if this spectral information were to play a role. This suggests that it is not even necessary that the photons have the same center wavelengths.

In conclusion, we have demonstrated a two-photon quantum interference effect in which the detected individual photons have quite different properties. Unlike other interference experiments, in which the photons themselves must be indistinguishable upon detection, the individual photons here have different polarization states, different arrival times, and different spectra. Indistinguishability still plays a critical role for quantum interference to occur, however, and comes in the form of the input state: For each detection event, there are essentially two possible sources (or quantum mechanical amplitudes) for the photon pair.

ACKNOWLEDGMENTS

This research was supported in part by the National Security Agency, the Advanced Research and Development Activity, and the Laboratory Directed Research and Development program of the Oak Ridge National Laboratory, managed for the U.S. Department of Energy by UT-Battelle, LLC, under contract DE-AC05-00OR22725. Y.-H. Kim also acknowledges support from the Korea Science and Engineering Foundation (R08-2004-000-10018-0), the Korea Research Foundation (KRF-2003-070-C00024), and POSTECH BSRI Research Fund-2004.

Y.-H. Kim's e-mail address is yoonho@postech.ac.kr.

REFERENCES AND NOTES

1. R. P. Feynman, R. Leighton, and M. Sands, *The Feynman Lectures on Physics*, Vol. III (Addison-Wesley, Reading, Mass., 1965).
2. R. P. Feynman, *QED The Strange Theory of Light and Matter* (Princeton U. Press, Princeton, N.J., 1985).
3. C. K. Hong, Z. Y. Ou, and L. Mandel, "Measurement of subpicosecond time intervals between two photons by interference," Phys. Rev. Lett. **59**, 2044–2046 (1987).
4. This photon bunching effect can also be observed as a peak in the two-photon detection rate; see Ref. 5.
5. Y.-H. Kim and W. P. Grice, "Observation of correlated-photon statistics using a single detector," Phys. Rev. A **67**, 065802 (2003).
6. This is sort of a quantum eraser operation. For discussions on quantum erasers, see Refs. 7 and 8.
7. M. O. Scully and K. Drühl, "Quantum eraser: a proposed photon correlation experiment concerning observation and 'delayed choice' in quantum mechanics," Phys. Rev. A **25**, 2208–2213 (1982).
8. Y.-H. Kim, R. Yu, S. P. Kulik, Y. Shih, and M. O. Scully, "Delayed choice quantum eraser," Phys. Rev. Lett. **84**, 1–5 (2000).
9. Y. H. Shih and C. O. Alley, in *Proceedings of the Second International Symposium on Foundations of Quantum Mechanics in the Light of New Technology*, M. Namiki, ed. (Physical Society of Japan, Tokyo, 1987).
10. Y. H. Shih and C. O. Alley, "New type of Einstein–Podolsky–Rosen–Bohm experiment using pairs of light quanta produced by optical parametric down conversion," Phys. Rev. Lett. **61**, 2921–2924 (1988).
11. Z. Y. Ou and L. Mandel, "Violation of Bells inequality and classical probability in a two-photon correlation experiment," Phys. Rev. Lett. **61**, 50–53 (1988).
12. P. G. Kwiat, A. M. Steinberg, and R. Y. Chiao, "Observation of a quantum eraser: a revival of coherence in a two-photon interference experiment," Phys. Rev. A **45**, 7729–7739 (1992).
13. D. V. Strekalov, T. B. Pittman, A. V. Sergienko, and Y. H. Shih, "Postselection-free energy-time entanglement," Phys. Rev. A **54**, R1–R4 (1996).
14. T. B. Pittman, D. V. Strekalov, A. Migdall, M. H. Rubin, A. V. Sergienko, and Y. H. Shih, "Can two-photon interference be considered the interference of two photons?" Phys. Rev. Lett. **77**, 1917–1920 (1996).
15. Y.-H. Kim, "Two-photon interference without bunching two photons," Phys. Lett. A **315**, 352–357 (2003).
16. Y.-H. Kim, M. V. Chekhova, S. P. Kulik, and Y. Shih, "Quantum interference by two temporally distinguishable pulses," Phys. Rev. A **60**, R37–R40 (1999).
17. Y.-H. Kim, "Measurement of one-photon and two-photon wave packets in spontaneous parametric downconversion," J. Opt. Soc. Am. B **20**, 1959–1966 (2003).
18. Y.-H. Kim, M. V. Chekhova, S. P. Kulik, Y. Shih, and M. H. Rubin, "First-order interference of nonclassical light emitted spontaneously at different times," Phys. Rev. A **61**, 051803(R) (2000).
19. Y.-H. Kim, V. Berardi, M. V. Chekhova, A. Garuccio, and Y. Shih, "Temporal indistinguishability and quantum interference," Phys. Rev. A **62**, 043820 (2000).
20. This particular scheme can be used to prepare polarization entangled photons when the pump is cw; see Ref. 21.
21. P. G. Kwiat, K. Mattle, H. Weinfurter, A. Zeilinger, A. V. Sergienko, and Y. H. Shih, "New high-intensity source of polarization-entangled photon pairs," Phys. Rev. Lett. **75**, 4337–4341 (1995).
22. With ultrafast pumps, as in this paper, polarization entangled photons cannot be obtained in general. See Refs. 23, 24, and 25.
23. T. E. Keller and M. H. Rubin, "Theory of two-photon entanglement for spontaneous parametric down-conversion driven by a narrow pump pulse," Phys. Rev. A **56**, 1534–1541 (1997).
24. W. P. Grice and I. A. Walmsley, "Spectral information and distinguishability in type-II down-conversion with a broadband pump," Phys. Rev. A **56**, 1627–1634 (1997).
25. Y.-H. Kim, S. P. Kulik, M. H. Rubin, and Y. Shih, "Comment on 'Dispersion-Independent high-visibility quantum interference in ultrafast parametric downconversion'," Phys. Rev. Lett. **86**, 4710 (2001).
26. Y.-H. Kim, S. P. Kulik, M. V. Chekhova, W. P. Grice, and Y. Shih, "Experimental entanglement concentration and universal Bell-state synthesizer," Phys. Rev. A **67**, 010301(R) (2003).
27. S. L. Braunstein and A. Mann, "Measurement of the Bell operator and quantum teleportation," Phys. Rev. A **51**, R1727–R1730 (1995).
28. Y.-H. Kim and W. P. Grice, "Reliability of the beam-splitterbased Bell-state measurement," Phys. Rev. A **68**, 062305 (2003).
29. Y.-H. Kim and W. P. Grice, "Generation of pulsed polarization-entangled two-photon state via temporal and spectral engineering," J. Mod. Opt. **49**, 2309–2323 (2002).
30. W. P. Grice, A. B. U'Ren, and I. A. Walmsley, "Eliminating frequency and space-time correlations in multiphoton states," Phys. Rev. A **64**, 063815 (2001).